Journal of Applied Mathematics and Physics, 2025, 13(11), 3780-3793
https://www.scirp.org/journal/jamp
ISSN Online: 2327-4379
ISSN Print: 2327-4352

Pattern Formations in Bacteria-Biosurfactant Interactions of Microbial Enhanced Oil Recovery

Sadrack Dingaonaro Mokein[1,2], Sali Issa[3*], Saidou Abdoulkary[4], Alidou Mohamadou[5], Henri Paul Ekobena Fouda[6]

[1]Department of Physics, Faculty of Science, University of Maroua, Maroua, Cameroon
[2]Department of Electrical Engineering, Faculty of Science, University of Doba, Doba, Tchad
[3]Department of Refining and Petrochemistry, National Advanced School of Mines and Petroleum Industries, University of Maroua, Maroua, Cameroon
[4]Department of Basic Science, National Advanced School of Mines and Petroleum Industries, University of Maroua, Maroua, Cameroon
[5]National Advanced School of Engineering of Maroua, University of Maroua, Maroua, Cameroon
[6]Laboratory of Biophysics, Department of Physics, Faculty of Science, University of Yaounde, Yaounde, Cameroon
Email: *issasali83@gmail.com

How to cite this paper: Dingaonaro Mokein, S., Issa, S., Abdoulkary, S., Mohamadou, A. and Ekobena Fouda, H.P. (2025) Pattern Formations in Bacteria-Biosurfactant Interactions of Microbial Enhanced Oil Recovery. *Journal of Applied Mathematics and Physics*, **13**, 3780-3793.
https://doi.org/10.4236/jamp.2025.1311211

Received: September 25, 2025
Accepted: November 7, 2025
Published: November 10, 2025

Abstract

This paper investigates the dynamic interactions between biosurfactant-producing bacteria and their environment through pattern formations in diffusive predator-prey models. By analyzing the model's equilibrium points and applying the Routh-Hurwitz criteria with bifurcation analysis, we determine the conditions for the existence of Turing patterns. Numerical simulations confirm these analytical findings and reveal diverse pattern formations influenced by diffusion and concentration zones, including both Turing and non-Turing patterns. We observe a correlation between the distribution of the two species through pattern formations and the effectiveness of biosurfactant-mediated oil recovery. More interestingly, our model focuses on the dynamics of bacterial and biosurfactant concentrations by showing that areas of high biosurfactant concentration are associated with the release of trapped oil from pores, thereby contributing to successful oil recovery.

Keywords

Two Specie Models, Predator-Prey Models, Pattern Formations, Spatial Diffusion

1. Introduction

Microbially Enhanced Oil Recovery (MEOR) utilizes microorganisms or their met-

abolic products such as biosurfactants, biopolymers, biomass, acids, solvents, gases and enzymes to increase oil recovery from depleted reservoirs, extending their lifespan. This concept, first suggested in 1926 by Beckman [1] and further studied by ZoBell in 1947 [2] [3], leverages microbial activity to alter fluid and rock properties within the reservoir. MEOR offers several advantages, including economic feasibility and environmental friendliness, as it utilizes biotechnology for enhanced oil recovery [4]. However, challenges remain, particularly in identifying microbial strains that can survive the extreme conditions as high temperature, pressure, salinity, and pH found in many reservoirs [5]. The main objective of MEOR is to modify fluid and rock properties to improve oil recovery. Biosurfactant-producing bacteria are particularly promising due to their biodegradability, tolerance to harsh conditions of temperature, pH and relative safety for humans. Even at low concentrations, these bacteria can produce effects comparable to chemical surfactants [6]. Several techniques have been proposed by researchers to enhance oil recovery, including *in-situ* MEOR techniques involve injecting water, microbes, and nutrients into the reservoir. This can improve rock permeability through the production of organic acids that dissolve the rock substrate and reduce interfacial tension (IFT) between oil and water by utilizing biosurfactants produced by the injected microorganisms [7]-[9].

Islam [10] proposed a mathematical model to describe microbial transport in multiphase, multidirectional flow through porous media. However, this model neglected the effects of physical dispersion represented by the actions of metabolic products. Experimental investigations in the MEOR process have characterized the optimal temperature and pH conditions for biosurfactant production by various bacteria, including *Clostridium* sp., *Geobacillus* strain, and *Bacillus* subtilis [11]-[13]. Sugai *et al.* [14] developed a mathematical model using a simulator to investigate MEOR processes involving polymer-producing microorganisms, utilizing laboratory data. Their findings indicated that increased water viscosity is the primary mechanism driving improved oil recovery. Motivated by these previous studies, we are developing and validating a predictive mathematical predator-prey model to describe the diffusive dynamics of bacterial growth and biosurfactant production. This model has the potential to significantly enhance our understanding and optimize the performance of MEOR mechanisms.

To the best of our knowledge, no previous studies have investigated the relationship or interaction between biosurfactant-producing bacterial growth and pattern formations, specifically focusing on the formation of strong concentration zones of two bacterial species. This study aims to address this gap by performing a numerical analysis of a reaction-diffusion system that considers the mobility of bacteria and biosurfactant with Fickian diffusion effects.

This work aims to elucidate the biological and mathematical implications of a model that more accurately describes bacterial growth, thereby contributing to the optimization of MEOR techniques. The primary focus is on identifying zones of high bacterial and biosurfactant concentration through pattern formations, in-

corporating diffusion effects. This analysis includes a detailed investigation of Turing instability conditions using the Routh-Hurwitz criteria to understand the stability dynamics of diffusive interactions between bacteria and biosurfactants. In the present work, we investigate the dynamics of a two-species model comprising bacteria and surfactant, focusing on the impact of diffusion on the stability of an improved prey-predator model. This paper is organized as follows: Section 2 presents a detailed description of the prey-predator model dynamics with two species in the presence of diffusion. Section 3 analyzes the local stability of the model. Section 4 is reserved for the bifurcation analysis through the diffusive model of MEOR system. Section 5 presents the results of multiple numerical simulations. Finally, Section 6 summarizes all the results.

2. Dynamic Models of MEOR System

The hypothesis of a biosurfactant producing bacteria in a reaction-diffusion framework through mathematical modifications of predator-prey models exploring the relationships of MEOR process through several biological products such as biosurfactant, biacid, biopolymer, biosolvent and gases has been developed by some previous works [15]-[17]. Assuming that mobility of the two species where the predator and prey are interacting towards each other obeys the Fickian diffusion, we consider a growth model of biosurfactant producing bacteria with possible movement of two species represented by bacteria population and biosurfactant density. This interaction can be interpreted as a toxic effect of biosurfactant on the bacterial population at high concentrations, which is commonly observed in biological systems where metabolic products can inhibit or kill the producers themselves. We propose the following system to describe biosurfactant producing bacteria growth with spatial dependence:

$$\begin{cases} \dfrac{\partial p}{\partial t} = \mu_1 p - \dfrac{\mu_1}{K_o} p^2 - \gamma ps + D_1 \nabla^2 p \\ -\dfrac{\partial s}{\partial t} = \mu_2 p - \delta ps + D_2 \nabla^2 s \end{cases} \tag{1}$$

where p is the number of bacteria in base-10 logarithm for each cell/mL, s is biosurfactant concentration (g/L), μ_1 is bacteria growth rate (h^{-1}), μ_2 is biosurfactant production rate (mg/cell/h), K_0 is carrying capacity (cell/mL), γ is toxicity constant (L/g/h), δ is predation factor (1/h) and The term $-\delta ps$ represents the degradation of biosurfactant due to bacterial activity. It simulates a process where bacteria consume or degrade the biosurfactant for their growth, a behavior often observed in microbial systems. $D_1 > 0$, $D_2 > 0$, which are respectively diffusion coefficients of the species p, s and $\nabla^2 = \dfrac{\partial}{\partial x^2} + \dfrac{\partial}{\partial y^2}$ is the Laplacian operator with the space variables x and y. This interaction can be interpreted as a toxic effect of biosurfactant on the bacterial population at high concentrations, which is commonly observed in biological systems where meta-

bolic products can inhibit or kill the producers themselves.

3. Local Stability Analysis

We investigate in this section the local stability analysis of biologically feasible equilibrium points by assuming that the non-diffusive model can be written as follows

$$\begin{cases} \dfrac{\mathrm{d}p}{\mathrm{d}t} = F(p,s) \\ \dfrac{\mathrm{d}s}{\mathrm{d}t} = G(p,s) \end{cases} \tag{2}$$

where

$$\begin{cases} F(p,s) = \mu_1 p - \dfrac{\mu_1}{K_o} p^2 - \gamma ps \\ G(p,s) = \mu_2 p - \delta ps \end{cases} \tag{3}$$

Clearly, the model (5) has trivial equilibrium point $E_0 = (0,0)$ and interior equilibrium point $E^* = (p^*, s^*)$, where $p^* = k_0\left(\mu_1 - \dfrac{\gamma}{\delta}\mu_2\right)$ and $s^* = \dfrac{\mu_2}{\delta}$. The interior equilibrium point E^* is biologically meaningful if p^*, s^* are nonnegative and we get the condition defined as $\mu_1 > \dfrac{\gamma}{\delta}\mu_2$.

The Jacobian matrix A_0 of the system (1) is

$$A_0 = \begin{bmatrix} F_p & F_s \\ G_p & G_s \end{bmatrix} = \begin{bmatrix} a_{11} & a_{12} \\ a_{21} & a_{22} \end{bmatrix}$$

where

$$\begin{cases} a_{11} = \mu_1 - 2\dfrac{\mu_1}{K_o} p^* - \gamma s^* \\ a_{12} = -\gamma p^* \\ a_{21} = \mu_2 - \delta s^* \\ a_{22} = -\delta p^* \end{cases} \tag{4}$$

The characteristic polynomial can be written as

$$\lambda^2 + \eta_1(0)\lambda + \eta_0(0) = 0 \tag{5}$$

where,

$$\begin{cases} \eta_1(0) = -(a_{11} + a_{22}) = -\mu_1 + 2\dfrac{\mu_1}{K_o} p^* + \gamma s + \delta p^* \\ \eta_0(0) = a_{11}a_{22} - a_{12}a_{21} = -\delta p^*\left(\mu_1 - 2\dfrac{\mu_1}{K_o} p^* - \gamma s\right) + \gamma p^*(\mu_2 - \delta s) \end{cases}$$

For second-degree polynomial, the Routh-Hurwitz criteria of the system (1) are stable if

$$\eta_1(0) > 0 \text{ and } \eta_0(0) > 0 \tag{6}$$

4. Bifurcation Analysis of MEOR System

It is well known that Turing's instability arises in a system because the uniform stationary state loses its stability due to scattering, dispersion or diffusion. In this section, we linearize the total system (1) around the state E^* for small temporal and spatial fluctuations, and the variables p and s are taken in Fourier space as

$$\begin{cases} p(\boldsymbol{x},t) \approx p^* + \Delta p(\boldsymbol{x},t), \\ s(\boldsymbol{x},t) \approx s^* + \Delta s(\boldsymbol{x},t) \end{cases} \tag{7}$$

where

$$\begin{cases} \left|\Delta p(\boldsymbol{x},t)\right| \ll p^*, \\ \left|\Delta s(\boldsymbol{x},t)\right| \ll s^*. \end{cases} \tag{8}$$

The perturbations $\Delta p(\boldsymbol{x},t)$ and $\Delta s(\boldsymbol{x},t)$ depend simultaneously on time and space of the following form:

$$\begin{cases} \Delta p(\boldsymbol{x},t) = \varepsilon_p \mathrm{e}^{\lambda} \mathrm{e}^{i\boldsymbol{k}\boldsymbol{x}}, \\ \Delta s(\boldsymbol{x},t) = \varepsilon_s \mathrm{e}^{\lambda} \mathrm{e}^{i\boldsymbol{k}\boldsymbol{x}} \end{cases} \tag{9}$$

with ε_p, ε_s representing constants. $\boldsymbol{x}$ is the space vector, $\boldsymbol{k}$ is the wave number vector with $k = |\boldsymbol{k}|$, λ represents the frequency of the wave and i is a complex number. By introducing Equation (7) in (1), we have

$$\begin{cases} \dfrac{\partial \Delta p}{\partial t} = a_{11}\Delta u + a_{12}\Delta s + D_1 \nabla^2 \Delta p, \\ \dfrac{\partial \Delta s}{\partial t} = a_{21}\Delta p + a_{22}\Delta s + D_2 \nabla^2 \Delta s. \end{cases} \tag{10}$$

Based on the precise form of Equation (9) and setting $|A_k - \lambda I| = 0$ where $A_k = A_0 - k^2 D$ and the diffusion matrix

$$D = \begin{bmatrix} D_1 & 0 \\ 0 & D_2 \end{bmatrix}$$

The characteristic equation of the model system is:

$$\lambda^2 + \eta_1(k)\lambda + \eta_0(k) = 0 \tag{11}$$

where

$$\begin{cases} \eta_1(k) = -(D_1 + D_2)k^2 + a_{11} + a_{22} \\ \eta_0(k) = D_1 D_2 k^4 - (D_1 a_{22} + D_2 a_{11})k^2 + a_{11}a_{22} \end{cases} \tag{12}$$

with

$$\begin{cases} a_{11} = \mu_1 - 2\dfrac{\mu_1}{K_0} p^* - \gamma s^* \\ a_{12} = -\gamma p^* \\ a_{21} = \mu_2 - \delta s^* \\ a_{22} = -\delta P^* \end{cases} \tag{13}$$

The roots of Equation (14) are:

$$\lambda = \frac{-\eta_1(k) \pm \sqrt{\eta_1^2(k) - 4\eta_0(k)}}{4\eta_1(k)} \tag{14}$$

The complete system (1) will be stable if all the Routh-Hurwitz criteria given by Equation (15) are respected

$$\eta_1(k) > 0 \text{ and } \eta_0(k) > 0 \tag{15}$$

for all *k*.

Violation of at least one of these previous stability conditions results in system instability caused by diffusion (*i.e.*, $Re(\lambda_k) > 0$). Turing's instability is induced by diffusion through the condition of internal equilibrium point if the non-diffusive local system is stable, and it will become unstable in the presence of diffusion. In fact, Turing instability will occur for system (1) if the conditions of inequality (6) are respected, but at least one of the conditions of inequalities (15) is not respected, *i.e.*, $Re(\lambda_k) < 0$ for $k = 0$ and $Re(\lambda_k) > 0$ for $k \neq 0$.

The location of the area for which the local system becomes asymptotically stable is very important for a study of Turing instability. Note here that for an appropriate choice of system parameters, the values of $\eta_1(0)$ and $\eta_0(0)$ can be positive.

To derive the criteria for diffusive instability of the model given by Equation (1). The system is unstable if one of the roots of the characteristic Equation (14) is positive. A necessary condition for one of the roots to be positive is $\eta_1(k) > 0$. So

$$\begin{cases} a_{11} + a_{22} > k^2(D_1 + D_2) \\ k^2 < \dfrac{a_{11} + a_{22}}{D_1 + D_2} \end{cases} \tag{16}$$

where *k* is the real positive wave number. We know that D_1 and D_2 are positive and real. Hence, the above equation is feasible only if $a_{11} > 0$ and $a_{22} > 0$. for $\eta_0(k) > 0$, we have

$$\begin{cases} F(k^2) = D_1 D_2 k^4 - (D_1 a_{22} + D_2 a_{11}) k^2 + a_{11} a_{22} > 0 \\ F(k^2) = F_2(k^2)^2 + F_1(k^2) + F_0 > 0 \end{cases} \tag{17}$$

The expression of Equation (17) is the function of k^2 and can be given in the following form $F(k^2)$.

The condition for having Turing instability in the system (1) is to have $F(k^2) < 0$ for at least one of these functions $\eta_0(k)$ or $\eta_1(k)$. The minimum Turing point are given by the following ratios

$$\frac{\partial F}{\partial k^2} = 0 \Rightarrow k^2 = -\frac{F_1}{2F_2} > 0 \tag{18}$$

where

$$F_1 = -(D_1 a_{22} + D_2 a_{11}) < 0 \text{ and } F_2 = D_1 D_2 > 0 \tag{19}$$

By setting the parameters as follows: $\gamma = 0.33$, $\delta = 0.08$, $\mu_1 = 0.09$, $\mu_2 = 0.54$

and, we obtain the values of the internal equilibrium point (0.2977, 0.0305) and the coefficients of dispersion given by $\eta_0(0) = -1.1404$, $\eta_1(0) = 0.3452$ which permit us to show that unstable of system (2) is related to the good choice of the value of the parameters. In order to better study the diffusive model (1), we plot the dispersion coefficient relations as a function of the wave number k in **Figures 1-4** with the graphical representation of the real part of Equation (14) for different values of the diffusion coefficients. We find that for certain values of k, $\eta_0(k) < 0$ and $\eta_1(k) > 0$, the Turing instability is possible because the Routh-Hurwitz criteria are violated, and inequalities (19) are satisfied. As shown in **Figure 2**, where the Routh-Hurwitz stability criteria are violated for certain values of the diffusion part of the curve is less than zero. We observe that these stability criteria are respected in **Figure 3**.

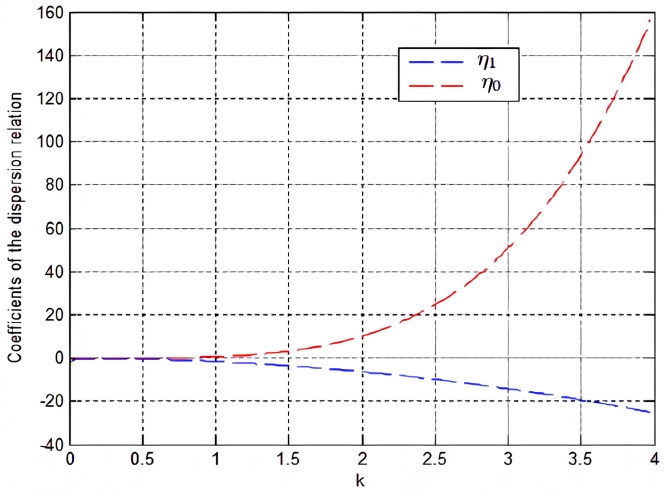

Figure 1. Coefficients of the dispersion relation. The parameters are taken as: $p = 1$; $s = 1$; $\mu_1 = 0.09$; $\gamma = 0.33$; $\mu_2 = 0.54$; $D_1 = D_2 = 0.02$.

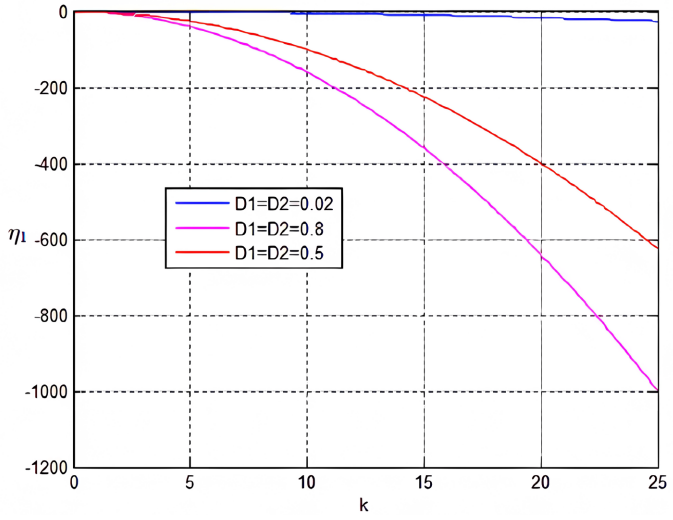

Figure 2. Coefficient of the dispersion relation. The parameters are taken as: $p = 1$; $s = 1$; $\mu_1 = 0.09$; $\gamma = 0.33$; $\mu_2 = 0.54$.

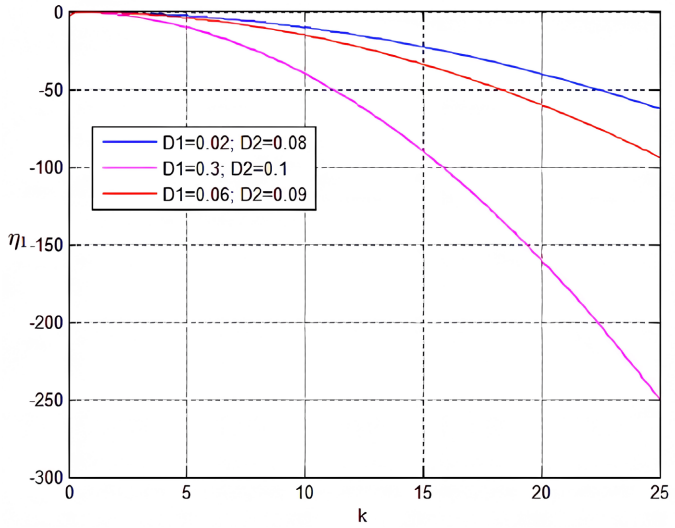

Figure 3. Coefficient of the dispersion relation. The parameters are taken as: $p = 1$; $s = 1$; $\mu_1 = 0.09$; $\gamma = 0.33$; $\mu_2 = 0.54$.

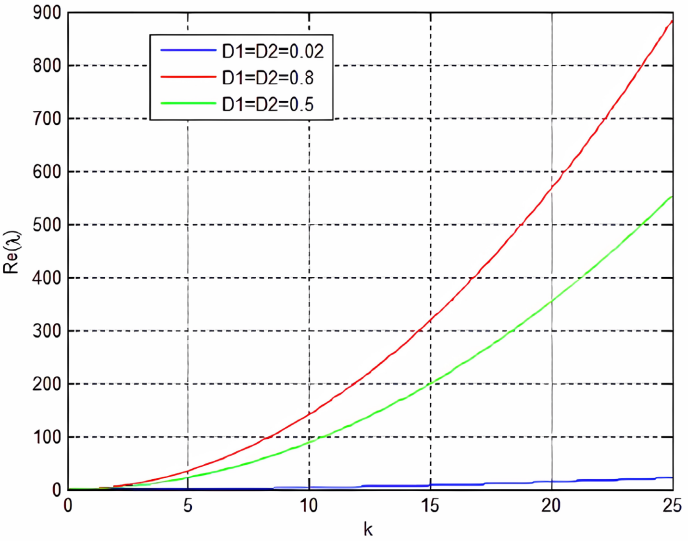

Figure 4. Coefficients of the dispersion relation. The parameters are taken as: $p = 1$; $s = 1$; $\mu_1 = 0.09$; $\gamma = 0.33$; $\mu_2 = 0.54$.

5. Numerical Experiments

We numerically solved the model system (1) in two-dimensional space within the finite domain [−100, 100] with initial conditions set near the equilibrium point E^*. To track the temporal evolution of the solution, we employed the Forward Euler method and a second-order central finite difference approximation to evaluate the diffusion term. This approach discretized the model in both time and space, following established techniques for solving PDE models [18]-[21]. We utilized a discrete domain with a grid of $Nx \times Ny$ units within the two-dimensional reaction-diffusion system. Initial conditions were randomly generated within the range [−0.5, 0.5], and zero-flux boundary conditions were applied. The

system was discretized using Euler's method with initial random conditions around the equilibrium state. By setting the time step $\Delta t = 0.085$ and the spatial step size $\Delta x = \Delta y = 0.04$, we investigated the influence of diffusion on pattern formation in our complete system. Varying the diffusion coefficients D_1 and D_2 allowed us to predict the spatial distribution of bacteria and biosurfactants within the well. We started by introducing a small perturbation around the internal equilibrium point $(0.2977, 0.0305)$ and we have represented the dynamic behaviors of species at different times $t = 1000$, $t = 5000$ and $t = 10000$. In the aim to bring out the diffusion effects in the dynamic localization of bacteria and biosurfactants in the system, we choose the numerical simulations parameters as follows $\mu_1 = 0.09$; $\gamma = 0.03$; $\mu_2 = 0.54$; $K_0 = 0.3$ and $\delta = 0.03$. We performed numerical simulations until the system reached a stable state, or at least until a stable pattern emerged. By increasing the diffusion coefficients respectively as $D_1 = D_2 = 0$; $D_1 = 0.06$ and $D_2 = 0.09$; $D_1 = 0.1$ and $D_2 = 0.3$, we observe pattern formations in Figures 5-10, which represent the densities of bacteria and biosurfactants in the well and determine his dynamic behavior. The number of small structure of patterns decrease with the amplitude by merging and become more and more localized through the illustrations of the bacteria specie p at different increasing times $t = 1000$, $t = 5000$ and $t = 10000$ in Figures 5-7 which illustrate the spatial patterns observed for the predator species p. We observe an increase in the number of patterns as the diffusion coefficient increases. These figures also

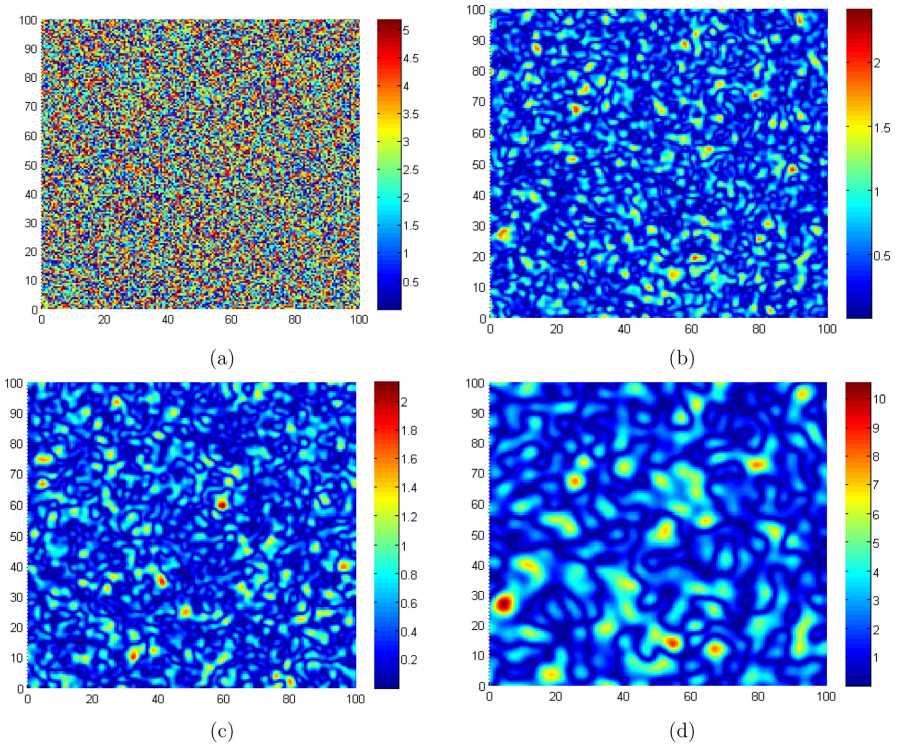

Figure 5. Panels show of the species p of model (1) for $t = 1000$. The parameters are taken as $\mu_1 = 0.09$; $\gamma = 0.03$; $\mu_2 = 0.54$; $K_0 = 0.3$; $\delta = 0.03$; (a) $D_1 = 0.0$, $D_2 = 0.0$. (b) $D_1 = 0.006$, $D_2 = 0.009$. (c) $D_1 = 0.02$, $D_2 = 0.08$. (d) $D_1 = 0.3$, $D_2 = 0.1$.

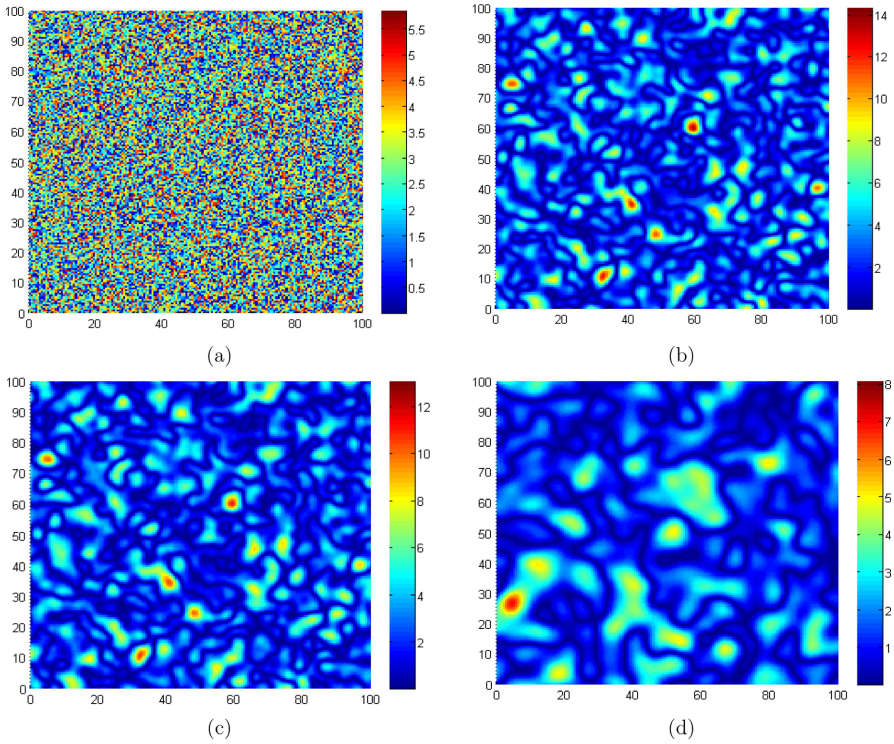

Figure 6. Panels show the species p of model (1) for $t = 5000$. The parameters are taken as $\mu_1 = 0.09$; $\gamma = 0.03$; $\mu_2 = 0.54$; $K_0 = 0.3$; $\delta = 0.03$; (a) $D_1 = 0.0$, $D_2 = 0.0$. (b) $D_1 = 0.006$, $D_2 = 0.009$. (c) $D_1 = 0.02$, $D_2 = 0.08$. (d) $D_1 = 0.3$, $D_2 = 0.1$.

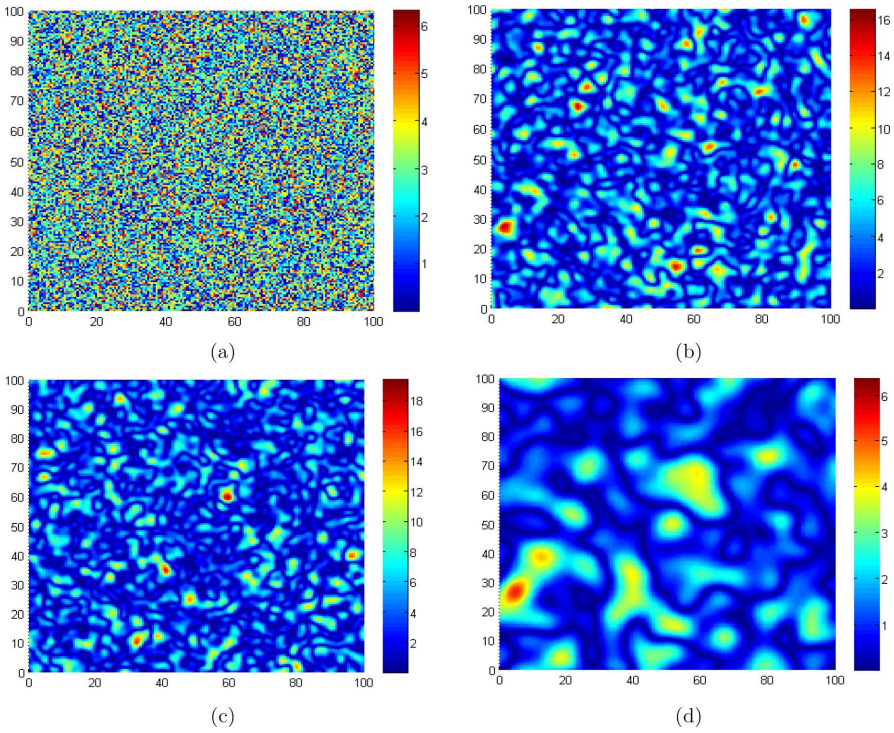

Figure 7. Panels show the species p of model (1) for $t = 10{,}000$. The parameters are taken as $\mu_1 = 0.09$; $\gamma = 0.03$; $\mu_2 = 0.54$; $K_0 = 0.3$; $\delta = 0.03$; (a) $D_1 = 0.0$, $D_2 = 0.0$. (b) $D_1 = 0.06$, $D_2 = 0.09$. (c) $D_1 = 0.02$, $D_2 = 0.08$. (d) $D_1 = 0.3$, $D_2 = 0.1$.

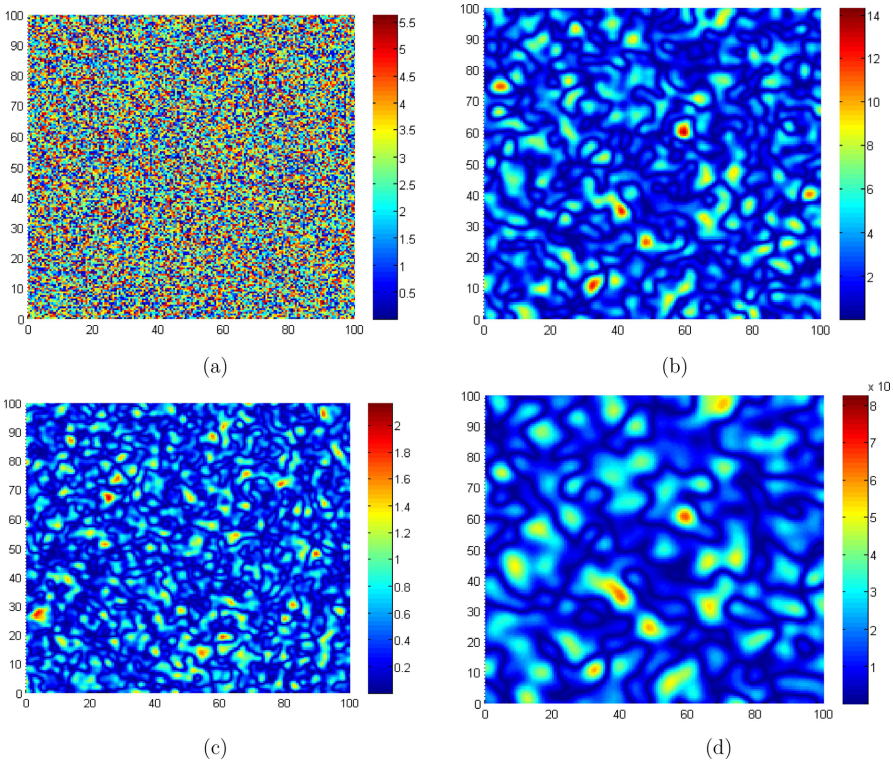

Figure 8. Illustration of the species s of model (1) for $t = 1000$. The parameters are taken as $\mu_1 = 0.09$; $\gamma = 0.03$; $\mu_2 = 0.54$; $K_0 = 0.3$; $\delta = 0.03$; (a) $D_1 = 0.0$, $D_2 = 0.0$. (b) $D_1 = 0.06$, $D_2 = 0.09$. (c) $D_1 = 0.02$, $D_2 = 0.08$. (d) $D_1 = 0.3$, $D_2 = 0.1$.

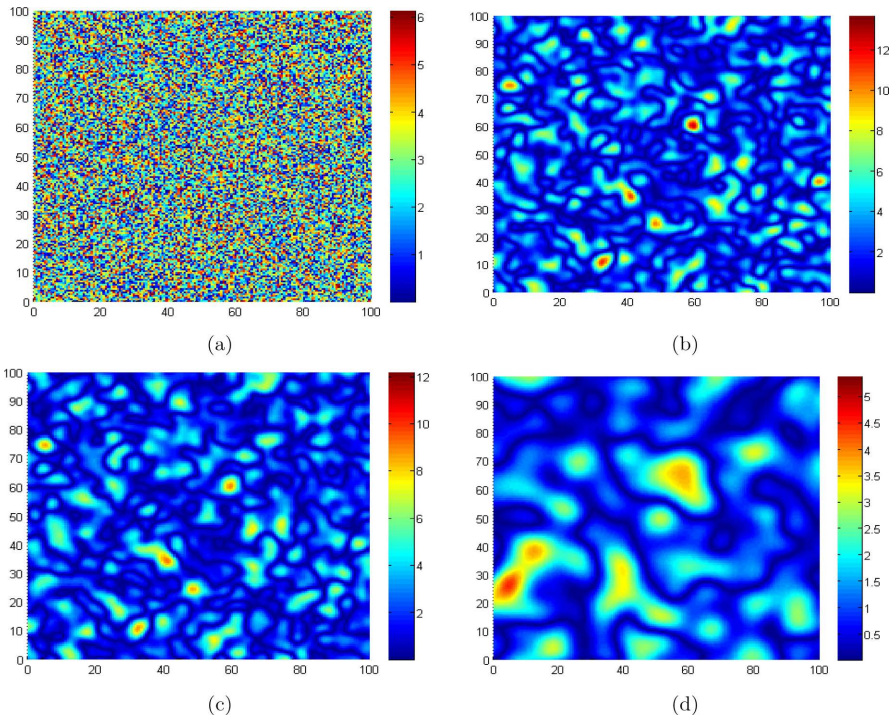

Figure 9. Illustration of the species s of model (1) for $t = 1000$. The parameters are taken as $\mu_1 = 0.09$; $\gamma = 0.03$; $\mu_2 = 0.54$; $K_0 = 0.3$; $\delta = 0.03$; (a) $D_1 = 0.0$, $D_2 = 0.0$. (b) D1 = 0.06, $D_2 = 0.09$. (c) $D_1 = 0.02$, $D_2 = 0.08$. (d) $D_1 = 0.3$, $D_2 = 0.1$.

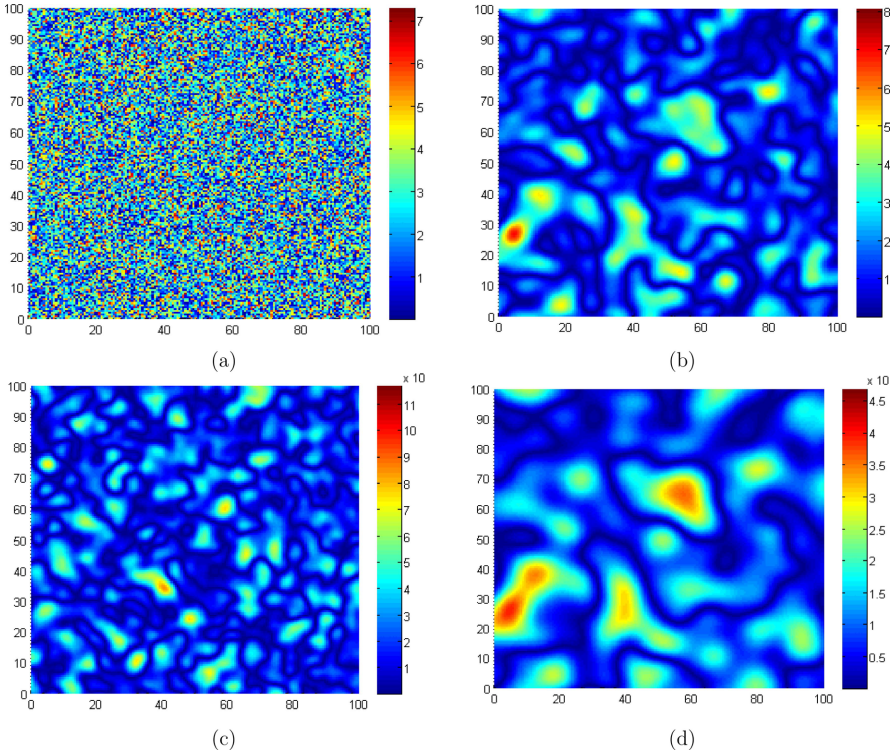

Figure 10. Illustration of the species s of model (1) for $t = 1000$. The parameters are taken as $\mu_1 = 0.09$; $\gamma = 0.03$; $\mu_2 = 0.54$; $K_0 = 0.3$; $\delta = 0.03$; (a) $D_1 = 0.0$, $D_2 = 0.0$. (b) $D_1 = 0.06$, $D_2 = 0.09$. (c) $D_1 = 0.02$, $D_2 = 0.08$. (d) $D_1 = 0.3$, $D_2 = 0.1$.

reveal dynamic behaviors, with spot types changing over time. Figures 8-10 depict the spatial patterns for the prey species s and by comparing to species p, we observe an increase in the number of pattern spots with increasing diffusion parameters. Diffusion can induce various pattern types when the local system is unstable, although these patterns exhibit limited temporal variation. By increasing diffusion terms and carefully selecting appropriate parameters, we can generate different types of Turing patterns. These patterns delineate areas of high bacterial and biosurfactant concentration. An increase in biosurfactant concentration zones is associated with the release of trapped oil from pores, leading to successful oil recovery. Our findings align with recent studies [3] [22] [23] and provide a framework for describing the dynamic interplay between biosurfactant and bacterial concentrations within the well using a diffusive predator-prey model.

6. Conclusion

This study investigates the impact of spatial diffusion on a two-species model involving bacteria and biosurfactant production. Our findings demonstrate that diffusion induces diverse pattern formations within the system and can destabilize the stable fixed points of the model. We analytically derived Turing conditions for pattern formation using the Routh-Hurwitz criterion and bifurcation analysis of the two-species model, incorporating diffusion parameters. Intensive numerical simulations were conducted, corroborating the analytical results and revealing a

wide range of pattern formations. A strong correlation was observed between the spatial distributions of bacteria and biosurfactant, characterized by the pattern formations describing the concentrated zones. More interestingly, our model focuses on the dynamics of bacterial and biosurfactant concentrations by showing that areas of high biosurfactant concentration are associated with the release of trapped oil from pores, thereby contributing to successful oil recovery. Our results provide valuable insights into the dynamics of bacteria and biosurfactant interactions within the well, offering a more comprehensive understanding based on diffusive predator-prey models. We acknowledge the limitations of the model, such as the assumption of homogeneity in the porous medium and the absence of nutrient dynamics modeling, and suggest that future research could integrate these aspects to improve the modeling of the MEOR process.

Conflicts of Interest

The authors declare no conflicts of interest regarding the publication of this paper.

References

[1] Beckmann, J.W. (1926) The Action of Bacteria on Mineral Oil. *Industrial and Engineering Chemistry, News Edition*, **4**, 23-26.

[2] ZoBell, C.E. (1947) Bacterial Release of Oil from Oil-Bearing Materials, Part I. *World Oil*, **126**, 36-47.

[3] Putra, W. and Hakiki, F. (2019) Microbial Enhanced Oil Recovery: Interfacial Tension and Biosurfactant-Bacteria Growth. *Journal of Petroleum Exploration and Production Technology*, **9**, 2353-2374. https://doi.org/10.1007/s13202-019-0635-8

[4] Sen, R. (2008) Biotechnology in Petroleum Recovery: The Microbial Eor. *Progress in Energy and Combustion Science*, **34**, 714-724. https://doi.org/10.1016/j.pecs.2008.05.001

[5] Youssef, N., Elshahed, M.S. and McInerney, M.J. (2009) Chapter 6. Microbial Processes in Oil Fields: Culprits, Problems, and Opportunities. In: *Advances in Applied Microbiology*, Elsevier, 141-251. https://doi.org/10.1016/s0065-2164(08)00806-x

[6] Patel, J., Borgohain, S., Kumar, M., Rangarajan, V., Somasundaran, P. and Sen, R. (2015) Recent Developments in Microbial Enhanced Oil Recovery. *Renewable and Sustainable Energy Reviews*, **52**, 1539-1558. https://doi.org/10.1016/j.rser.2015.07.135

[7] Sivasankar, P. and Suresh Kumar, G. (2017) Improved Empirical Relations for Estimating Original Oil in Place Recovered during Microbial Enhanced Oil Recovery under Varied Salinity Conditions. *Petroleum Science and Technology*, **35**, 2036-2043. https://doi.org/10.1080/10916466.2017.1378676

[8] Behesht, M., Roostaazad, R., Farhadpour, F. and Pishvaei, M.R. (2008) Model Development for MEOR Process in Conventional Non-Fractured Reservoirs and Investigation of Physico-Chemical Parameter Effects. *Chemical Engineering & Technology*, **31**, 953-963. https://doi.org/10.1002/ceat.200800094

[9] Armstrong, R.T. and Wildenschild, D. (2012) Microbial Enhanced Oil Recovery in Fractional-Wet Systems: A Pore-Scale Investigation. *Transport in Porous Media*, **92**, 819-835. https://doi.org/10.1007/s11242-011-9934-3

[10] Islam, M.R. (1990) Mathematical Modeling of Microbial Enhanced Oil Recovery. *SPE*

Annual Technical Conference and Exhibition, New Orleans, September 1990, 23-26. https://doi.org/10.2118/20480-ms

[11] Arora, P., Ranade, D.R. and Dhakephalkar, P.K. (2014) Development of a Microbial Process for the Recovery of Petroleum Oil from Depleted Reservoirs at 91 - 96˚C. *Bioresource Technology*, **165**, 274-278. https://doi.org/10.1016/j.biortech.2014.03.109

[12] Sun, S., Zhang, Z., Luo, Y., Zhong, W., Xiao, M., Yi, W., *et al.* (2011) Exopolysaccharide Production by a Genetically Engineered Enterobacter Cloacae Strain for Microbial Enhanced Oil Recovery. *Bioresource Technology*, **102**, 6153-6158. https://doi.org/10.1016/j.biortech.2011.03.005

[13] Vaz, D.A., Gudiña, E.J., Alameda, E.J., Teixeira, J.A. and Rodrigues, L.R. (2012) Performance of a Biosurfactant Produced by a *Bacillus* Subtilis Strain Isolated from Crude Oil Samples as Compared to Commercial Chemical Surfactants. *Colloids and Surfaces B*: *Biointerfaces*, **89**, 167-174. https://doi.org/10.1016/j.colsurfb.2011.09.009

[14] Sugai, Y., Hong, C., Chida, T. and Enomoto, H. (2004) Simulation Studies on the Mechanisms and Performances of MEOR Using a Polymer Producing Microorganism *Clostridium* sp. TU-15A. *Asia Pacific Oil and Gas Conference and Exhibition*, **69**, 335-347.

[15] Fernandes, P.L., Rodrigues, E.M., Paiva, F.R., Ayupe, B.A.L., McInerney, M.J. and Tótola, M.R. (2016) Biosurfactant, Solvents and Polymer Production by *Bacillus* Subtilis RI4914 and Their Application for Enhanced Oil Recovery. *Fuel*, **180**, 551-557. https://doi.org/10.1016/j.fuel.2016.04.080

[16] Joshi, S., Bharucha, C. and Desai, A.J. (2008) Production of Biosurfactant and Antifungal Compound by Fermented Food Isolate *Bacillus* Subtilis 20b. *Bioresource Technology*, **99**, 4603-4608. https://doi.org/10.1016/j.biortech.2007.07.030

[17] Gudiña, E.J., Pereira, J.F.B., Rodrigues, L.R., Coutinho, J.A.P. and Teixeira, J.A. (2012) Isolation and Study of Microorganisms from Oil Samples for Application in Microbial Enhanced Oil Recovery. *International Biodeterioration & Biodegradation*, **68**, 56-64. https://doi.org/10.1016/j.ibiod.2012.01.001

[18] Mitchell, A. and Griffiths, D. (1980) The Finite Difference Method in Partial Differential. Wiley.

[19] Ames, W.F. (1992) Numerical Methods for Partial Differential Equations. Academic Press.

[20] Murray, J.D. (2003) Mathematical Biology II Spatial Models and Biomedical Applications. Vol. 18, 3rd Edition, Springer.

[21] Shaikh, T.S., Fayyaz, N., Ahmed, N., Shahid, N., Rafiq, M., Khan, I., *et al.* (2021) Numerical Study for Epidemic Model of Hepatitis-B Virus. *The European Physical Journal plus*, **136**, Article No. 367. https://doi.org/10.1140/epjp/s13360-021-01248-8

[22] Hakiki, F. (2014) A Critical Review of Microbial Enhanced Oil Recovery Using Artificial Sand-Stone Core: A Mathematical Model. 38*th Annual Convention and Exhibition of Indonesian Petroleum Association*, Jakarta, 21-23 May 2014, IPA14-SE-119.

[23] Mincheva, M. and Roussel, M.R. (2012) Turing-Hopf Instability in Biochemical Reaction Networks Arising from Pairs of Subnetworks. *Mathematical Biosciences*, **240**, 1-11. https://doi.org/10.1016/j.mbs.2012.05.007